

# Pickering-Emulsion-Templated Encapsulation of a Hydrophilic Amine and Its Enhanced Stability Using Poly(allyl amine)

Jun Li,<sup>†</sup> Andrew D. Hughes,<sup>‡</sup> Tom H. Kalantar,<sup>§</sup> Ian J. Drake,<sup>‡</sup> Chris J. Tucker,<sup>§</sup> and Jeffrey S. Moore<sup>\*†</sup>

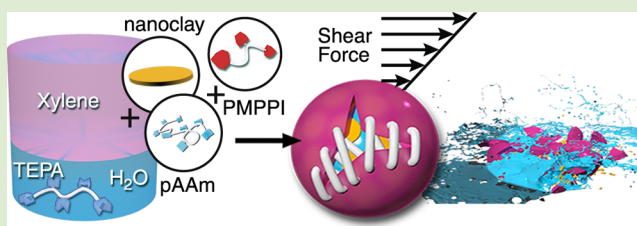
<sup>†</sup>Department of Chemistry and the Beckman Institute of Advanced Science and Technology, University of Illinois at Urbana–Champaign, Urbana, Illinois 61801, United States

<sup>‡</sup>Department of Core – Formulations Science, The Dow Chemical Company, Spring House, Pennsylvania 19477, United States

<sup>§</sup>Department of Core – Formulations Science, The Dow Chemical Company, Midland, Michigan 48674, United States

## S Supporting Information

**ABSTRACT:** Efficient encapsulation of tetraethylenepentamine (TEPA), as an example aliphatic amine, was achieved by an emulsion-templated, in situ polymerization. Hydrophobically modified clay nanoplatelets were employed as emulsifiers to obtain water-in-oil (W/O) dispersions followed by interfacial polymerization between a portion of the TEPA cargo and polymethylene polyphenylene isocyanate (PMPPi). The resultant capsules exhibit spherical shape, desirable thermal stability, modest barrier properties, and shear-induced release in an epoxide monomer mixture. Most importantly, a significant gain in capsule barrier properties was realized by introducing poly(allyl amine) (pAAm) as an interface-selective reactive additive in the Pickering emulsions. In addition to the fundamental interest of pAAm localization and interface-selective reactivity, this microencapsulation system for aliphatic amines has technological potential in coating, self-healing, and drug-delivery applications.



Synthetic coatings are ubiquitously applied on architectures ranging from bridges to skyscrapers to provide protection against corrosion and corrosive failure.<sup>1,2</sup> Epoxy, as one of the most widely used industrial protective coatings, is a bicomponent coating material, consisting of glycidyl ether monomer (epoxy resin) and hardener.<sup>3</sup> Aliphatic amines are the most common hardener because they can initiate curing without catalyst under ambient conditions. Compared to aromatic amines, incorporation of aliphatic amines also imparts distinctive benefits to the final coating such as being less susceptible to photodegradation and oxidation during usage.<sup>4,5</sup> However, aliphatic amines can present environmental, health, and safety issues when stored unpackaged: acute and chronic toxicity, carcinogenicity, and odor are major concerns.<sup>6,7</sup> It is therefore desirable to develop a premixed epoxy coating system, so as to avoid on-site handling of concentrated amines, minimize stoichiometric errors, and simplify the coating process. Deactivation of the amine component and mixing it directly with epoxy resin for later on-demand activation<sup>8</sup> is an ideal approach. Encapsulation is an especially enticing deactivation method because rapid release of the curing agent is possible through a variety of triggers;<sup>9</sup> however, aliphatic amines have proven to be especially difficult payloads to encapsulate.<sup>10,11</sup> The miscibility of aliphatic amines with water and organic solvents frustrates efforts to emulsify and partition them with good fidelity. These challenges interfere with the standard method for encapsulation by interfacial polymerization or formalin deposition methods.<sup>12–14</sup>

Among a variety of encapsulation techniques differing in active cargos<sup>15–17</sup> or modalities,<sup>18–21</sup> colloidal particle-stabilized droplets, known as “Pickering emulsions”, have emerged as a promising approach toward liquid-core microcapsule formation.<sup>22,23</sup> Like surfactant-stabilized emulsions, Pickering emulsions<sup>24,25</sup> are either oil-in-water (O/W) or water-in-oil (W/O) dispersions, the latter of which are referred to as inverse Pickering emulsions. Very broadly, Pickering emulsions are stabilized by hydrophilic particles,<sup>25–29</sup> while inverse Pickering emulsions result when hydrophobic particles are used.<sup>30–32</sup> On the basis of these Pickering emulsion templates, various shell matrix fabrication techniques are of use for encapsulations.<sup>33,34</sup> Polar liquid core components (e.g., amines) have presented a particularly difficult target for conventional shell formation methods including radical polymerization and layer-by-layer (LBL) assembly.<sup>29,35</sup> The former is hindered by chain transfer tendencies, while the latter is impeded by polar active interference of ionic interactions. Recently, interfacial condensation polymerization between multifunctional amines and isocyanates was utilized as an alternative shell-formation method to circumvent these challenges and encapsulate nonpolar actives and aromatic amines as payloads.<sup>36–38</sup>

Herein, we demonstrate efficient encapsulation of the aliphatic amine tetraethylenepentamine (TEPA) via an inverse Pickering emulsion. Partitioning of the aliphatic amine into the

Received: July 25, 2014

Accepted: September 4, 2014

Published: September 10, 2014

organic phase was abated by the use of a nonpolar organic solvent and addition of water, which helped drive the amine into the polar phase. Using hydrophobically modified clay nanoplatelets as a stabilizer, the sequential interfacial polymerization between polymethylene polyphenylene isocyanate (PMPPI) and TEPA, with concurrent encapsulation of TEPA, was achieved. The resultant capsules displayed high thermal stability and moderate chemical stability when mixed with epoxide monomers. The premixed suspension exhibited rapid curing upon mechanical activation. Viscosity drift on the time scale of hours indicated the need for capsules with improved barrier properties. The encapsulation method was then improved by the addition of poly(allyl amine) (pAAm) as a remarkably effective interfacial-selective chemical cross-linker for the shell, which enhanced the stability of microcapsules suspended in liquid epoxide monomers.

The nonspecific partitioning of the aliphatic amine TEPA was alleviated by emulsification with nonpolar solvent (e.g., xylene) and a small amount of water. The concentration of aliphatic amines in the continuous nonpolar phase as a function of water addition was monitored using gas chromatography–mass spectrometry (GC–MS) with dodecane as an internal standard. TEPA was replaced with diethylenetriamine (DETA) in these experiments because DETA showed a single-peak signal in gas chromatography. Various amounts of water were added to premixed DETA–xylene solutions (1:10 mass ratio), resulting in a biphasic liquid, the organic layer of which was subjected to GC–MS analysis. As shown in Figure 1a, the

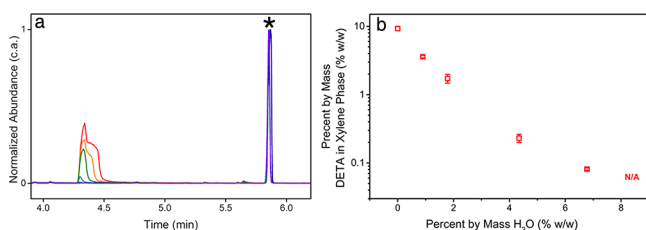
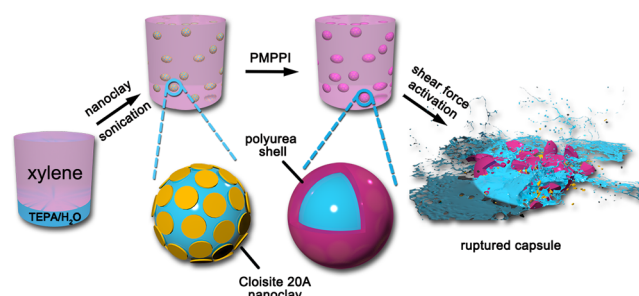


**Figure 1.** (a) GC–MS trace of DETA dissolved in xylenes with internal standard dodecane indicated by \* (0%, red; 0.90%, orange; 1.78%, green; 4.35%, cyan; 6.78%, blue; 8.33%, violet; percent by mass of H<sub>2</sub>O) and (b) percent by mass of DETA distributed in the xylene phase versus addition of water.

abundance of DETA (retention time = 4.28 min) in the nonpolar phase continuously decreased with increasing water content. The decrease of DETA in the xylene phase upon volume change of the polar phase was quantified using an internal standard and a calibration curve (Figure 1b and Figure S1, Supporting Information). Beyond ca. 8 wt % water addition, the amount of DETA that remained in the nonpolar xylenes phase fell below the detection limit. The addition of water significantly drives the amine out of the organic phase and therefore confines the subsequent encapsulation reaction between TEPA and PMPPI to the oil–water interface (vide infra).

As shown in Scheme 1, hydrophobically modified clay nanoplatelets (Cloisite 20, Figure S2, Supporting Information) were used to stabilize the biphasic mixture of xylenes and TEPA in water. This mixture generated an inverse Pickering emulsion upon sonication, which displayed remarkable stability against coalescence and maintained its morphology in the subsequent in situ polymerization step (Figure S3, Supporting Information, and vide infra). Interfacial polymerization was conducted by

### Scheme 1. Illustration of Encapsulation and Activation Steps<sup>a</sup>



<sup>a</sup>PMPPI is the polymeric isocyanate polymethylene polyphenylene isocyanate while TEPA is tetraethylenepentamine.

introducing the polymeric isocyanate polymethylene polyphenylene isocyanate (PMPPI) into the fresh Pickering emulsion. After quenching the residual isocyanates with excess bis(2-ethylhexyl)amine (Figure S4, Supporting Information), the polyurea-shelled capsules containing amine and water at the core were obtained. The clay nanoplatelets are most likely incorporated into the shell wall during the interfacial polymerization, possibly increasing the robustness of the capsule.<sup>39</sup> The amine capsules rupture under high shear force, releasing the encapsulated TEPA for potential applications including curing of an epoxide monomer (Scheme 1 and vide infra).

Microcapsules with an average diameter ca. 18  $\mu\text{m}$  resulted from the encapsulation route described above, and their morphology was characterized using optical and fluorescence microscopy as shown in Figure 2. Spherical microcapsules with a narrow size distribution were observed using bright-field mode (Figure 2a). The core was visualized by incorporating fluorescein isothiocyanate (FITC, in a molar ratio to TEPA of 0.09%) into the payload (Figure 2b and Figure S5, Supporting

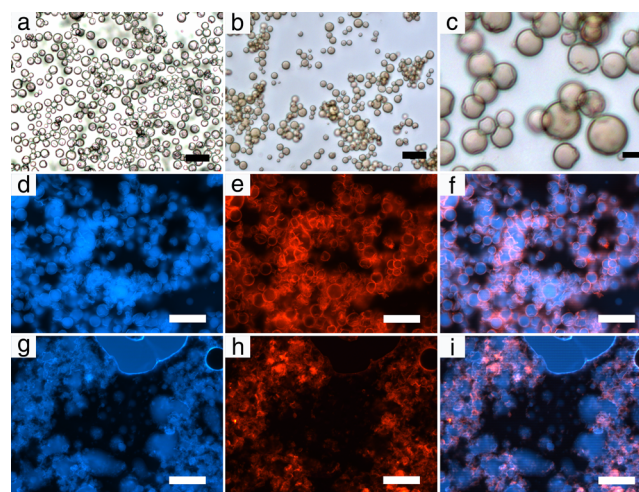


**Figure 2.** Optical micrographs of (a) TEPA/water microcapsules with a polyurea shell wall, (b) FITC-payload-stained TEPA/water microcapsules (scale bar is 10  $\mu\text{m}$  in c). Fluorescence micrographs of intact capsules with (d) FITC-stained core, (e) rhodamine 6G-stained shell wall, and (f) merged image. Fluorescence micrographs of ruptured capsules after activation using a high shear force homogenizer with (g) FITC-stained core, (h) rhodamine 6G-stained shell wall, and (i) merged image. All scale bars are 50  $\mu\text{m}$  unless otherwise specified.

Information), and the shell was visualized by PMPPI pretreated with Rhodamine 6G (see the Supporting Information for experimental details).

The morphology of the FITC-derivatized microcapsules was further imaged using fluorescence microscopy. The FITC-stained core is seen as discrete blue fluorescent spherical objects (Figure 2d), while the capsule walls stained with rhodamine 6G reveal a clear red ring of shell material (Figure 2e). Combining the two images, we observed red rings surrounding the blue spheres indicating the desired amine core was encapsulated within the shell walls (Figure 2f). When high shear force was applied using a homogenizer probe at 167 Hz for 60 s, the red rings of shell material became less defined (Figure 2h), and the core liquid agglomerated, indicating it was released (Figure 2g). The rupture of capsules is especially apparent in the merged image (Figure 2i), wherein the rhodamine 6G-stained shell material randomly overlaps with the FITC-stained core liquids, indicating that the capsule structure was destroyed.

A dynamic thermal TGA experiment, following an isothermal protocol<sup>40</sup> (Figure 3a, blue line), was employed to examine the

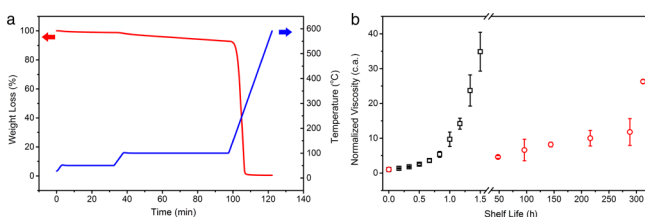


**Figure 3.** (a) Representative isothermal TGA curves of TEPA/water core capsules (a, red line) plotted versus the temperature profile (a, blue line): ramped from 30 to 50 °C at 10 °C min<sup>-1</sup>, kept at 50 °C for 30 min, ramped from 50 to 100 °C at 10 °C min<sup>-1</sup>, kept at 100 °C for 60 min, and then ramped to 650 °C at 10 °C min<sup>-1</sup>. Comparison of the normalized viscosity change between premixed neat TEPA/DER 331 epoxy monomer (b, black square) and microencapsulated TEPA/DER 331 epoxy monomer composite (b, red circle).

thermal stability of TEPA-loaded microcapsules. Generally, the microcapsules were heated to 50 °C and incubated at that temperature for 30 min in order to eliminate residual solvents. Then the temperature was raised and held at 100 °C for 1 h to examine the thermal stability and permeability of the TEPA-loaded capsules. The microcapsules maintained a stable weight in the isothermal step at 100 °C, which indicated good thermal stability and limited permeability of the core contents through the microcapsules (Figure 3a, red line). When ramped to 650 °C, the microcapsules presented a sharp weight loss starting from around 150 °C, consistent with thermal decomposition of the shell wall material (Figure S6, Supporting Information), and loss of capsule barrier properties.

The TEPA-loaded microcapsules were also stable when suspended in liquid epoxide monomer DER 331 (2,2'-(((propane-2,2-diylbis(4,1-phenylene))bis(oxy))bis(methylene))-bis(oxirane)). In contrast to the microcapsule suspension, a mixture of neat TEPA and DER 331 epoxide monomer solidifies within 1.5 h (Figure 3b, black square). Before the system hardened, the final viscosity measurement was 34 times that of the initial viscosity (denoted as normalized viscosity). For comparison, the polyurea-barrier-separated microencapsulated TEPA exhibited limited permeability when suspended in DER 331. Normalized viscosity of the suspension remained under 4 times after 24 h of storage and 12 times after 300 h of storage (Figure 3b, red circle).

Transport of the amine out of the microcapsules is very likely the consequence of diffusion of the payload through the shell wall during storage, considering the relative dearth of pinhole defects in capsules synthesized using interfacial polymerization.<sup>41</sup> Typically, incorporating a chemical cross-linker is an effective method to slow diffusion through polymers. Thus, poly(allyl amine) (pAAm) (molecular weight = 17k Da) was introduced into the polar phase during emulsion formation for subsequent participation in the interfacial polymerization. Remarkably, even at low loadings of pAAm, significant improvement of the shelf life of the TEPA-loaded microcapsules-DER 331 epoxide monomer suspension was observed (vide infra).

As shown in Figure 4a, addition of pAAm with concentration of 5 mg/mL or higher in water considerably decreased the rate

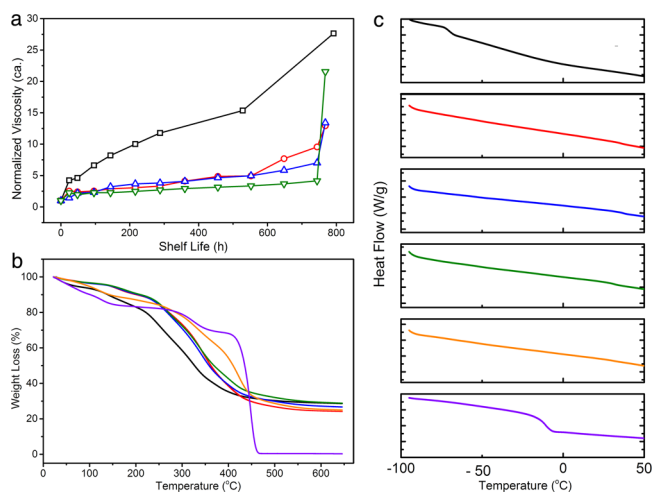


**Figure 4.** (a) Viscosity change of TEPA-loaded microcapsules and DER 331 epoxy suspension at different loadings of pAAm varying from 0 to 25 mg/mL in water (0 mg/mL, black; 5 mg/mL, red; 10 mg/mL, blue; 25 mg/mL, green). (b) TGA and (c) DSC curves of shell materials with different loading of pAAm varying from 0 to 25 mg/mL in water and pure product from pAAm and PMPPI; pAAm polymer as controls (0 mg/mL, black ( $T_g = -74.51$  °C)); 5 mg/mL, red; 10 mg/mL, blue; 25 mg/mL, green; pure product of pAAm and PMPPI, orange; pAAm polymer, purple,  $T_g = -11.72$  °C).

of undesirable TEPA release, so that the normalized viscosity of the suspension remained below 5 after 500 h of storage (Figure 4a). It is worth mentioning that the lowest dosage of pAAm (5 mg/mL) was 1% weight of TEPA, whose concentration was 500 mg/mL in water. The extension of shelf life was further improved when the pAAm concentration was raised to 25 mg/mL or higher. High shear force was applied at 744 h, and the resulting sharp increase in viscosity indicated the TEPA and DER 331 were still reactive upon pAAm addition. The effect of pAAm molecular weight and the use of other additives on the microcapsules are discussed in the Supporting Information.

We wondered how such a small quantity of pAAm leads to drastic improvements. To investigate the mechanism by which pAAm enhances shelf life, a series of thermal analyses were conducted on the shell wall materials of pAAm-dosed microcapsules, which were ground and washed to remove soluble contents. Thermogravimetric analysis (TGA) displayed a clear shift to higher decomposition temperatures for the capsule shell materials dosed with pAAm (Figure 4b). A solid product was made from pAAm solution and PMPPI as a

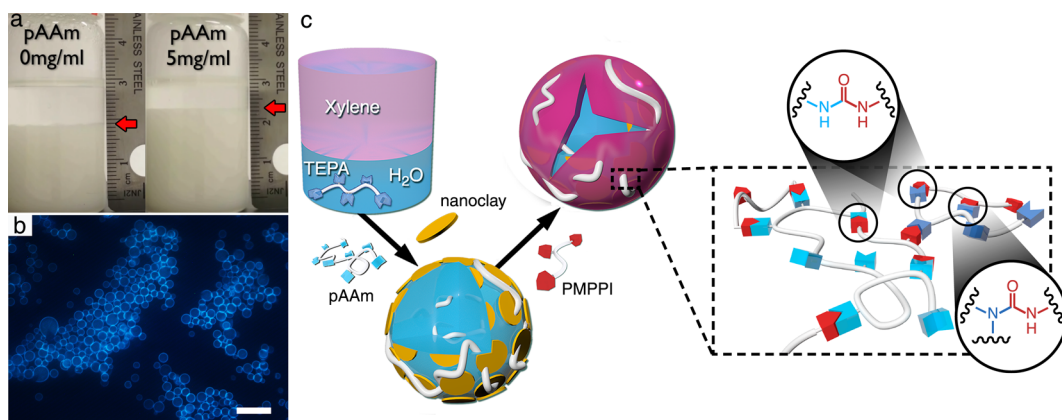


**Figure 5.** (a) Snapshot at 20 min after Pickering emulsion was generated (red arrows pointing to the interface of supernatant and emulsion bulk). (b) Fluorescence microscope images of 5 mg/mL of FITC-tagged-pAAm-dosed microcapsules (scale bar 50  $\mu\text{m}$ ). (c) A possible mechanism illustrating pAAm aggregation at the interface of the generated emulsion and subsequent cross-linking into the capsule shell.

reference, and the thermal degradation of the resultant material took place at a higher temperature (Figure 4b, orange line). Similar differences in thermal properties were observed when the shell materials were characterized using differential scanning calorimetry (DSC). A distinct glass transition peak ca.  $-75\text{ }^{\circ}\text{C}$  (Figure 4c, black line), which is typical for soft segments in polyurea,<sup>42</sup> disappeared in the presence of even the lowest loadings of pAAm (Figure 4c, red, blue, and green lines), corresponding to the DSC curve of shell material formed merely from pAAm and PMPPI (Figure 4c, orange line). The vanishing of a glass transition peak was assigned to decreased mobility of the network segments in the shell material, presumably as a result of cross-linking due to pAAm incorporation.

The addition of pAAm not only decreased the release of TEPA when capsules were suspended in DER 331 epoxy but also improved the stability of the initial Pickering emulsion as evidenced by the slower settling rate (Figure 5a). This enhanced stability may derive from the pAAm localized at the droplet interface, stabilizing the emulsion droplets as a macromolecular surfactant. The surface localization was observed by fluorescently tagging the pAAm polymer (Figure S9, Supporting Information) and characterizing the material with fluorescence microscopy. The images show pAAm prefers to migrate to the interface as indicated by a distinct blue ring at the edge of each emulsion droplet (Figure S10, Supporting Information) and capsule (Figure 5b). This result is in contrast to the TEPA-FITC adduct which did not concentrate in the capsule shell (Figure 2d) despite TEPA also acting as the shell-forming monomer (vide supra).

On the basis of these observations, we propose a mechanism that postulates the localization of pAAm at the emulsion droplet interface and the subsequent improvement in performance of pAAm containing TEPA capsules (Figure 5c). In the absence of pAAm, a fundamental difficulty facing aliphatic amine encapsulation using interfacial polymerization is the dual role of the amine as shell former and payload. TEPA is in gross stoichiometric excess (200 times) over the PMPPI isocyanate macromonomer in molar terms and even more so when comparing the relative abundance of reactive functional groups on each molecule (TEPA has five amino groups; the PMPPI has 2.7 isocyanate groups). Considering the emulsion's overall composition, the molar differential between TEPA and PMPPI greatly disfavors extended polymer formation, as each incoming

isocyanate group could readily react with an unreacted TEPA. The lack of extended polymer formation is supported by the presence of a low-temperature  $T_g$  in the pAAm free samples (Figure 4C, black line). Were the TEPA and PMPPI reacting with a closer molar equivalence, the resulting polyurea network would be almost completely cross-linked, and no  $T_g$  should be visible. The apparently high surface activity of pAAm in the emulsion phase differentiates it from TEPA and allows it to preferentially react with an incoming isocyanate macromonomer. Forcing the polymerization between the relatively few pAAm molecules and the PMPPI insures a greater degree of polymerization and network formation with fewer dangling ends.

Mediated by hydrophobically modified clay nanoplatelets, the efficient encapsulation of an aliphatic amine was accomplished using Pickering emulsion-templated interfacial polymerization. The resultant microcapsules exhibited satisfactory thermal stability and were formulated into an epoxy resin to afford a stable suspension with a modest shelf life that could be cured by rupturing the capsules using mechanical force. The stability of the amine-loaded microcapsules was considerably improved with the addition of linear polyamine pAAm, an additive that appears to be interfacially active, thereby improving the stoichiometric efficiency of the shell-forming reaction. Future efforts will address the mechanistic details, and we intend to exploit the procedure to prepare aliphatic amine-loaded microcapsules in different sizes and shell wall thicknesses for potential applications in protective coatings and self-healing materials.<sup>43,44</sup>

## ■ ASSOCIATED CONTENT

### 📄 Supporting Information

1. Emulsion formation methods; 2. Optical micrograph of Pickering emulsions; 3. Other miscellaneous information. This material is available free of charge via the Internet at <http://pubs.acs.org>.

## ■ AUTHOR INFORMATION

### Corresponding Author

\*E-mail: [jsmoore@uiuc.edu](mailto:jsmoore@uiuc.edu).

### Notes

The authors declare no competing financial interest.

## ■ ACKNOWLEDGMENTS

This work was supported by the Dow Chemical Company through Grant RPS 226772 AA. The authors would like to thank Keith Harris and Joshua Katz of the Dow Chemical Company for helpful discussion and facilitating the collaboration. The authors would also like to thank Southern Clay Products, Inc., and Nittobo Medical Co., Ltd. and Kenko Corporation for courtesy cloisite 20a and poly(allyl amine) samples, respectively.

## ■ REFERENCES

- (1) Gray, J. E.; Luan, B. J. *Alloys Compd.* **2002**, 336, 88–113.
- (2) Stern, K. H. *Metallurgical and ceramic protective coatings*; Springer: New York, 1996.
- (3) Qian, M.; Soutar, A. M.; Tan, X. H.; Zeng, X. T.; Wijesinghe, S. L. *Thin Solid Films.* **2009**, 517, 5237–5242.
- (4) Dyakonov, T.; Mann, P. J.; Chen, Y. *Polym. Degrad. Stab.* **1996**, 54, 67–83.
- (5) Mailhot, B.; Morlat-Thérias, S.; Ouahioune, M.; Gardette, J. L. *Macromol. Chem. Phys.* **2005**, 206, 575–584.
- (6) Weisburger, E. K.; Russfield, A. B.; Homburger, F. J. *Environ. Pathol. Toxicol.* **1977**, 2, 325–356.
- (7) Greim, H.; Bury, D.; Klimisch, H. J.; Oeben-Negele, M.; Ziegler-Skylakakis, K. *Chemosphere* **1998**, 36, 271–295.
- (8) Yin, T.; Rong, M. Z.; Zhang, M. Q.; Yang, G. C. *Compos. Sci. Technol.* **2007**, 67, 201–212.
- (9) Esser-Kahn, A. P.; Sottos, N. R.; White, S. R.; Moore, J. S. *J. Am. Chem. Soc.* **2010**, 132, 10266–10268.
- (10) McIlroy, D. A.; Blaiszik, B. J.; Caruso, M. M.; White, S. R.; Moore, J. S.; Sottos, N. R. *Macromolecules* **2010**, 43, 1855–1859.
- (11) Esser-Kahn, A. P.; Odom, S. A.; Sottos, N. R.; White, S. R.; Moore, J. S. *Macromolecules* **2011**, 44, 5539–5553.
- (12) Brown, E. W.; Kessler, M. R.; Sottos, N. R.; White, S. R. *J. Microencapsulation* **2003**, 20, 719–730.
- (13) Cui, J.; Wang, Y.; Postma, A.; Saulnier, P. *Adv. Funct. Mater.* **2010**, 20, 1625–1631.
- (14) Kobašlija, M.; McQuade, D. T. *Macromolecules* **2006**, 39, 6371–6375.
- (15) Poe, S. L.; Iija, M. K.; McQuade, D. T. *J. Am. Chem. Soc.* **2007**, 129, 9216–9221.
- (16) Städler, B.; Price, A. D.; Chandrawati, R.; Hosta-Rigau, L.; Zelikin, A. N.; Caruso, F. *Nanoscale* **2009**, 1, 68–73.
- (17) White, S. R.; Sottos, N. R.; Geubelle, P. H.; Moore, J. S.; Kessler, M. R.; Sriram, S. R.; Brown, E. N.; Viswanathan, S. *Nature* **2001**, 409, 794–797.
- (18) Immordino, M. L.; Dosio, F.; Cattel, L. *Int. J. Nanomed.* **2006**, 1, 297–315.
- (19) Discher, D. E.; Eisenberg, A. *Science* **2002**, 297, 967–973.
- (20) Jansen, J. F. G. A.; de Brabander-van den Berg, E. M. M.; Meijer, E. W. *Science* **1994**, 266, 1226–1229.
- (21) Douglas, T.; Young, M. *Nature* **1998**, 393, 152–155.
- (22) Kosif, I.; Cui, M.; Russell, T. P.; Emrick, T. *Angew. Chem., Int. Ed.* **2013**, 52, 6620–6623.
- (23) Pickering, S. U. *J. Chem. Soc., Trans* **1907**, 91, 2001–2021.
- (24) Binks, B. P.; Lumsdon, S. O. *Langmuir* **2000**, 16, 8622–8631.
- (25) Böker, A.; He, J.; Emrick, T.; Russell, T. P. *Soft Matter* **2007**, 3, 1231–1248.
- (26) Duan, H.; Wang, D.; Kurth, D. G.; Möhwald, H. *Angew. Chem., Int. Ed.* **2004**, 43, 5639–5642.
- (27) Cha, J. N.; Birkedal, H.; Euliss, L. E.; Bartl, M. H.; Wong, M. S.; Deming, T. J.; Stucky, G. D. *J. Am. Chem. Soc.* **2003**, 125, 8285–8289.
- (28) Melle, S.; Lask, M.; Fuller, G. G. *Langmuir* **2005**, 21, 2158–2162.
- (29) Li, J.; Hitchcock, A. P.; Stöver, H. D. *Langmuir* **2010**, 26, 17926–17935.
- (30) Dinsmore, A. D.; Hsu, M. F.; Nikolaidis, M. G.; Marquez, M.; Bausch, A. R.; Weitz, D. A. *Science* **2002**, 298, 1006–1009.
- (31) Lin, Y.; Skaff, H.; Emrick, T.; Dinsmore, A. D.; Russell, T. P. *Science* **2003**, 299, 226–229.
- (32) Voorn, D. J.; Ming, W.; van Herk, A. M. *Macromolecules* **2006**, 39, 2137–2143.
- (33) Grigoriev, D. O.; Bukreeva, T.; Möhwald, H.; Shchukin, D. G. *Langmuir* **2008**, 24, 999–1004.
- (34) Zhang, K.; Wu, W.; Guo, K.; Chen, J.; Zhang, P. *Langmuir* **2010**, 26, 7971–7980.
- (35) Zhang, Y.; Yang, S.; Guan, Y. *Macromolecules* **2003**, 36, 4238–4240.
- (36) McIlroy, D. A.; Blaiszik, B. J.; Caruso, M. M.; White, S. R.; Moore, J. S.; Sottos, N. R. *Macromolecules* **2010**, 43, 1855–1859.
- (37) Li, J.; Mazumder, M. A.; Stöver, H. D.; Hitchcock, A. P.; Shirley, I. M. *J. Polym. Sci., Part A: Polym. Chem.* **2011**, 49, 3038–3047.
- (38) Hickey, J.; Burke, N. A.; Stöver, H. D. *J. Membr. Sci.* **2011**, 369, 68–76.
- (39) Bon, S. A. F.; Colver, P. J. *Langmuir* **2007**, 23, 8316–8322.
- (40) Yang, Y.; Wei, Z.; Wang, C.; Tong, Z. *ACS Appl. Mater. Interfaces* **2013**, 5, 2495–2502.
- (41) Li, J.; Hitchcock, A. P.; Stöver, H. D.; Shirley, I. *Macromolecules* **2009**, 42, 2428–2432.
- (42) Primeaux, D. J. *Polyurea elastomer technology: history, chemistry & basic formulating techniques [J]*; Primeaux Associates LLC: Texas, 2004.
- (43) Jin, H.; Mangun, C. L.; Stradley, D. S.; Moore, J. S.; Sottos, N. R.; White, S. R. *Polymer* **2012**, 53, 581–587.
- (44) Caruso, M. M.; Blaiszik, B. J.; White, S. R.; Sottos, N. S.; Moore, J. S. *Adv. Funct. Mater.* **2008**, 18, 1898–1904.